FATIGUE FAILURE IN LINEARLY VISCOELASTIC MATERIALS

M. L. Williams
Professor of Engineering
University of Utah

W. G. Knauss
Assistant Professor
Firestone Flight Sciences Laboratory
California Institute of Technology

F. R. Wagner
Assistant Research Professor
College of Engineering
University of Utah

ABSTRACT

The thermodynamic approach to the fracture of linearly viscoelastic materials presented earlier is extended to include fatigue. The theoretical analysis of the growth of an internal spherical flaw due to a uniformly distributed, oscillatory input of displacement in the radial direction predicts a growth-rest type of flaw growth which depends upon the properties of the media and the loading frequency. Comparison of these results with experimental crack growth data for a pre-cracked sheet specimen subjected to an oscillatory displacement input discloses a qualitative similarity in behavior. It is, therefore, believed that the analytical model employed is representative of real flaw behavior and that its study can reveal the main features of macroscopic flaw-growth.

INTRODUCTION

At the International Conference on Fracture held in Sendai, Japan, we presented a formulation of the fracture problem for linearly viscoelastic materials based upon the energy balance concept.[1,2] The approach is similar to that employed by Griffith[3] in studying fracture of brittle materials, but includes the appropriate terms for viscous energy dissipation.

Now whereas it is in principle possible to predict the behavior in an arbitrary crack configuration, e.g. a Griffith[3] or Sneddon[4] type flaw, the relative mathematical complexity for these geometries is considerable, particularly when compounded with the viscoelastic time dependence. For analytical purposes, it is therefore desirable to find a flaw configuration whose analysis is relatively simple yet whose behavior is similar to real crack behavior. Derivation of the critical stresses for various flaw configurations in an elastic media yielded

A substantial portion of the work reported herein was supported by the National Aeronautics and Space Administration under Research Grant No. NsG 172-60 and Contract No. NGR-45-003-029.

TABLE I. ELASTIC FRACTURE STRESSES

Flaw Geometry	Critical Stress
2-D Crack (Griffith)	$\sqrt{2/\pi}\ \sqrt{ET/a_o}$
Cylindrical Cavity (a/b→0)	$\sqrt{2/2}\ \sqrt{ET/a_o}$
3-D Crack (Sneddon)	$\sqrt{2\pi/3}\ \sqrt{ET/a_o}$
Spherical Cavity (a/b→0)	$4/3\ \sqrt{ET/a_o}$

Note that although the stress analysis for the cylindrical and spherical flaws are much simpler, the elastic fracture stress expressions are functionally similar and are even quantitatively comparable.* Encouraged by the above, it is hypothesized that a similar comparison will exist for viscoelastic media. The study of viscoelastic fracture may thus be conducted with considerable simplification by using the cylindrical or spherical flaw geometry. All analysis in this paper assumes a spherical flaw of initial radius a_o and loaded in hydrostatic tension at radius b.

The Sendai paper presented the failure calculations for four different loading histories: constant stress (creep), constant strain (stress relaxation), constant stress rate, and constant strain rate. For example, the time to failure, t_f, under constant stress was found to be determined by:

TABLE II. TIME TO FAILURE FOR CREEP LOADING

Flaw Geometry	Stress State	Failure Criterion, a/b→0
Cylindrical cavity	Equi-biaxial	$\sigma_{critical} = 2/\sqrt{2}\ \sqrt{(T/a_o)/(2D_{crp}(t_f)-D_g}$
Spherical cavity	Hydrostatic tension	$\sigma_{critical} = 4/3\ \sqrt{(T/a_o)/(2D_{crp}(t_f)-D_g}$

$D_{crp}(t)$, creep compliance, psi^{-1}; $D_g = D_{crp}(0)$, glassy compliance.

This paper extends the results of the Sendai paper to include the case of failure under repeated loading of a general linearly viscoelastic material. Results for a three element model were presented previously.[5] Thus it is possible to predict fatigue crack initiation and growth in linearly viscoelastic materials.

THERMODYNAMIC CRITERION

Neglecting any energy dissipation in the form of kinetic energy or permanent (plastic) deformation, the conservation of energy concept requires that

$$\dot{I} = \dot{F} + 2\dot{D} + \dot{SE} \qquad (1)$$

* In the derivation of the cylinder and sphere expressions, it is assumed that the increase in fracture surface area is uniformly distributed around the periphery of the flaw. Although this is probably not true, this hypothesis does not appear to markedly affect numerical results.

where $\dot{I}$ is the power input of the applied loading at the boundary, $\dot{F}$ is the rate of increase of the free (strain) energy, 2D is the dissipation (mechanical power converted into heat flow), and $\dot{SE}$ is the rate of increase of surface energy (the dot over a symbol denotes differentiation with respect to time). Specifically, one has

$$\dot{I} = \int_A \overset{\nu}{T}_i \, \dot{u}_i \tag{2}$$

where $\overset{\nu}{T}_i$ are the components of the stress vector on the surface, A, and

$$\dot{F} + 2D = \frac{d}{dt} \int_{vol} \int_o^t \sigma_i \dot{\varepsilon}_i \, dt \, d(vol) \tag{3}$$

$$\dot{SE} = \frac{d}{dt} \int_A T \, dA \tag{4}$$

where T is the energy required to produce one unit of new surface area.

The stress distribution around a spherical flaw of radius a(t), such that $a(0) = a_0$, in an elastic media which is subjected to hydrostatic tension $\sigma_0 f(t)$ at radius r = b, is given by[6]

$$\sigma_r(r,t) = \sigma_0 f(t) \, \frac{1-\alpha(a_o^3/r^3)}{1-\alpha k^3} \tag{5}$$

$$\sigma_\phi(r,t) = \sigma_\theta(r,t) = \sigma_0 f(t) \, \frac{1+(\alpha/2)(a_o^3/r^3)}{1-\alpha k^3} \tag{6}$$

where

$$\alpha(t) \equiv \left[a(t)/a_0\right]^3; \quad k \equiv a_0/b \tag{7}$$

Since the stress distribution is independent of the material properties (also characteristic of the stresses around a cylindrical flaw), the solution for a viscoelastic media can be obtained by application of the Laplace transform analogy.[7] Thus it is possible to show that the infinitesimal strains for a linearly viscoelastic, isotropic, incompressible, homogeneous material are

$$\varepsilon_r(r,t) = -2\varepsilon_\theta(r,t) = \frac{\sigma_0}{r^3} \left\{ D_g S(t) + \int_o^t \frac{\partial D_{crp}(t-\tau)}{\partial(t-\tau)} \, S(\tau) \, d\tau \right\} \tag{8}$$

where S(t) is a cavity-size, load history dependent function defined as

$$S(t) = -\frac{3}{2} \, \frac{a^3(t) \, f(t)}{1-\left[a(t)/b\right]^3} \tag{9}$$

and the material behavior is described by the creep compliance $D_{crp}(t)$. Substitution of (5) thru (8) into the energy equation (1) yields the following condition for cavity growth

$$\dot{a} \left\{ -\frac{\sigma_0^4}{a^4} \int_o^t S(\xi) \, \frac{\partial}{\partial \xi} \left[D_g S(\xi) + \int_o^\xi \frac{\partial D_{crp}(\xi-\tau)}{\partial(\xi-\tau)} \, S(\tau) \, d\tau \right] d\xi + 2aT \right\} = 0 \tag{10}$$

Note that this condition is satisfied if $\dot{a} = 0$ or if the quantity in the brackets is zero. The former is the condition of a stationary flaw and holds up to the fracture initiation time, i.e. $\dot{a}(t) = 0$ for $t < t_f$. The latter is an integral expression for $a(t)$ and describes the propagating flaw, i.e. $t > t_f$.

In a similar manner, the assumption of a displacement loading $u(b,t) = u_0 g(t)$ leads to the condition

$$\dot{a}\left\{\frac{4b^6}{a^4}\left(\frac{u_0}{b}\right)^2 \int_0^t \frac{\partial g(\xi)}{\partial \xi}\left[E_g g(\xi) + \int_0^\xi \frac{\partial E_{rel}(\xi-\tau)}{\partial(\xi-\tau)} g(\tau)d\tau\right] d\xi - 2aT\right\} = 0 \quad (11)$$

where $E_{rel}(t)$ is the relaxation modulus, $E_{rel}(0) \equiv E_g$, and the obvious stationary solution $\dot{a}(t) = 0$ as well as the condition for a propagating flaw are again obtained.

FATIGUE FAILURE

Consider now the case of a sinusoidally applied displacement, i.e. $g(t) = \sin \omega t$. Since we desire the non-stationary solution we set the bracketed quantity of (11) to zero. Integrating the first term and rearranging produces

$$\frac{T}{2a}\left(\frac{a}{b}\right)^6\left(\frac{b}{u_0}\right)^2 = \frac{E_g}{2} g^2(t) + \int_0^t \frac{\partial g}{\partial \xi}\int_0^\xi \frac{\partial E_{rel}(\xi-\tau)}{\partial(\xi-\tau)} g(\tau)\, d\tau\, d\xi \quad (12)$$

which if $g(0) = 0$ as in this case, can be expressed in the equivalent form

$$\frac{T}{2a}\left(\frac{a}{b}\right)^6\left(\frac{b}{u_0}\right)^2 = \int_0^t \frac{\partial g}{\partial \xi}\int_0^\xi \frac{\partial g(\nu)}{\partial \nu} E_{rel}(\xi-\nu)d\nu\, d\xi \quad (13)$$

Now it is desirable to introduce a specific representation for the relaxation modulus. The expression used here is

$$E_{rel}(t) = E_e + \sum_{i=1}^{N} E_i \exp(-t/\tau_i) \quad (14)$$

which has been shown to be capable of fitting experimental stress relaxation data with a sufficient degree of accuracy.[8] The material description is thus general. Substituting (14) into (13) and integrating yields

$$\frac{T}{2a}\left(\frac{a}{b}\right)^6\left(\frac{b}{u_0}\right)^2 = \frac{E_e}{4}(1 - \cos 2\omega t) + \sum E_i\left\{\frac{\omega\tau_i}{1+\omega^2\tau_i^2}\left[\frac{\omega t}{2} + \frac{\sin 2\omega t}{4}\right]\right.$$
$$+ \frac{\omega^2\tau_i^2}{1+\omega^2\tau_i^2}\left[\exp^{-t/\tau_i} \cos \omega t - 1\right] \quad (15)$$
$$\left. - \frac{\omega^3\tau_i^3}{(1+\omega^2\tau_i^2)^2}\left[\exp^{-t/\tau_i} \sin \omega t\right]\right.$$

$$+ \frac{\omega^2\tau_i^2}{4(1+\omega^2\tau_i^2)} \left[1 - \cos 2\omega t\right] \Bigg\} \qquad \text{(15 contd.)}$$

which is the thermodynamic condition for determining the flaw size variation with time, $a(t) \geq a_0$ for $t > t_f$.

ILLUSTRATIVE EXAMPLE

Figure 1 shows a plot of equation (15) for Solithane 113 cyclically loaded at a rate of 5.4 cps. A seven element representation for the relaxation modulus was used, i.e. N = 7 in equation (14) where E_e = 558.0 psi and

τ_i	E_i, psi
10^{-1}	108.17
10^{-2}	208.62
10^{-3}	5664.1
10^{-4}	16491
10^{-5}	23743
10^{-6}	25303
10^{-7}	22357

The ordinate of Figure 1 is proportional to the fifth power of the flaw radius and the abscissa is time. The figure, therefore, illustrates that portion of flaw behavior associated with flaw size variation. For the complete picture of flaw growth during fatigue, the stationary flaw solution $\dot{a} = 0$ must also be considered.

We interpret the results in the following manner: Until the flaw size predicted by equation (15) equals the initial flaw size, the stationary flaw solution governs and the flaw will not grow, i.e. $a(t) = a_0$ for $t \leq t_f$ (see Figure 2). At $t = t_f$ the flaw begins to increase in size following a path predicted by the non-stationary solution of the general thermodynamic power equation (equation (15)). Note, however, that this solution undergoes a series of local maxima immediately after which the flaw is predicted to decrease in size and then increase until it reaches a new maximum larger than the first. This behavior must be examined in light of its physical significance. For a flaw to exhibit this behavior, it would be necessary for the crack to reheal or bond itself back together. This is highly unlikely for the new surfaces tend to remain separated once a crack has developed. This means that once the flaw grows to one of the local maxima it will remain at that size (stationary solution governing) until the non-stationary solution reaches and exceeds that value. The flaw will then grow until it reaches a new maximum. In this manner, a fatigue crack will propagate in a series of growth and rest periods until the flaw can no longer accommodate the applied load by deformation alone, and rapid fracture occurs. This stop-start behavior is illustrated in Figure 2.

EXPERIMENTAL RESULTS

The foregoing calculations should be viewed as a qualitative indication of the motion of a crack in a cyclic strain field. Because the growth of a crack in an infinite medium (the geometry considered in the above calcula-

tions) changes the stress magnitudes, if not the stress distribution around the flaw, the growth rate depends on the current flaw size. If we neglect this flaw size dependence as embodied essentially in the fifth power dependence of the flaw radius on time (cf Fig. 2), we are left with the jump or stop-start propagation of a flaw. Let us now compare this growth behavior with experimental results obtained in a geometry which eliminates the dependence on flaw size. The specimen used in previous crack propagation studies [8,9] is shown inset in Figures 3 and 4.

The material employed was Solithane 113, made up of equal parts by volume of catalyst and prepolymer.[10] The strain history applied to the specimen was a sinusoidal strain of magnitude ε superposed on a constant prestrain of magnitude ε. Note that in the calculations the prestrain is equal to zero.

The results of the two tests are shown in Figures 3 and 4. The difference in the two is the strain level. Figure 3 presents data for a maximum strain of 20% and Figure 4 for 25%. In both cases the prestrain was one-half the maximum. For the low strain ε_{max} = 20%, the rate of crack propagation is not as uniform and regular as the calculations indicate. This deviation may be attributed to the influence of local variations in material properties where small variations become less important at higher strains and higher crack velocities. This is evident when one looks at Figure 4 which is the results of prescribing a strain of value ε_{max} = 25%.

The fracture progressed faster at the larger strain level and there were not as many cycles before failure was noted. Notwithstanding the differences between the theoretical model and the flaw configuration tested, the actual crack propagation in a start-stop or stepped fashion which resembles the behavior predicted (see Figure 2).

The data were obtained by photographing the advancing crack with a Hycam variable speed camera (5 to 10,000 frames per second) and each point plotted corresponds to one frame. Note that in Figure 4 some points seem to be missing. The reason for this data gap is that it was hard to determine the location of the crack tip because the crack was almost closed at that time. Because this condition corresponds to zero strain, the data gaps locate conveniently the beginning and end of one complete cycle.

Note furthermore that although the timescale (zero on the time scale was unintentionally shifted on Figure 4 by about 0.12 sec) indicates the length of a cycle, the beginning of the complete cycle from zero strain through the maximum strain and back to zero strain begins at 0.12 sec. At that time the velocity of crack propagation is zero, increasing rapidly to its maximum near the peak strain and then reaches zero again.

CONCLUSIONS

Although the theoretical prediction was based upon a three-dimensional stress field in which the fracture surface is assumed equally distributed over the flaw surface and a simple sinusoidal loading whereas the experimental study was conducted on a two-dimensional configuration using a superimposed prestrain and sinusoidal strain variation, a qualitative similarity between the actual and predicted flaw behavior has been demonstrated. This is deemed significant for two reasons. First, the predicted growth-rest cycle of crack

propagation has been demonstrated and secondly, the results tend to substantiate the hypothesis that there is a close association between the spherical flaw geometry with its uniformly distributed new surface generation and an actual sharp pointed crack. The latter will greatly simplify the study of macroscopic crack propagation in viscoelastic media.

While the above is encouraging, a quantitative correlation is highly desirable. This should follow additional experimental verification, such as is in progress for the sheet specimen previously employed. Furthermore, it should be emphasized that the theoretical development presented here does not include the effects of (1) variations from equal triaxial loading, (2) finite strains, (3) compressibility, and (4) explicit consideration of a crack rather than smooth flaw fracture geometry. The present results, however, are believed to furnish a useful guide for investigating fracture initiation and growth in linearly viscoelastic media.

REFERENCES

1. M. L. Williams, "Initiation and Growth of Viscoelastic Fracture," International Journal of Fracture Mechanics, Vol. 1, No. 4, December 1965, pp. 292-310.

2. W. G. Knauss, "Time Dependent Fracture of Viscoelastic Materials," Proceedings of the International Conference on Fracture, Sendai, Japan, September 1965.

3. A. A. Griffith, "The Theory of Rupture," Proceedings of the First International Congress of Applied Mechanics, Delft, 1924, pp. 55-63.

4. I. N. Sneddon, "The Distribution of Stress in the Neighborhood of a Crack in an Elastic Solid," Proceedings of the Royal Society (London), Series A, Vol. 187, October 1946.

5. M. L. Williams, "Fracture in Viscoelastic Media," paper presented at the Ilikon Corporation Symposium held in Boston, Mass., January 31 - February 1, 1966.

6. S. Timoshenko and J. N. Goodier, Theory of Elasticity, 2nd ed., New York: McGraw-Hill Book Co., Inc., 1959, pp. 358-359.

7. M. L. Williams, "Structural Analysis of Viscoelastic Materials," AIAA Journal, Vol. 2, No. 5, May 1964, pp. 405-411.

8. R. A. Schapery, "Approximate Methods of Transform Inversion for Viscoelastic Stress Analysis," Proceedings of the Fourth U. S. National Congress of Applied Mechanics, Vol. 2, 1962, p. 1075.

9. W. G. Knauss, "Rupture Phenomena in Viscoelastic Materials," Ph.D. Dissertation, California Institute of Technology, June 1963.

10. W. G. Knauss, "On the Propagation of Failure in a Biaxial Stress Field," Working Group on Mechanical Behavior, Bulletin of the Third Meeting, Interagency Chemical Rocket Propulsion Group, Vol. 1, October 1964, pp. 437-454.

11. W. G. Knauss, "A Cross-Linked Polymer Standard Report on Polymer Selection," First Annual Report on AF Contract No. AF 04(611)-9572, AFRPL-TR-65-111, April 1965. MATSCIT PS 65-3, California Institute of Technology.

12. W. G. Knauss, J. F. Clauser, and R. F. Landel, "Second Report on the Selection of a Cross-Linked Polymer Standard," Annual Report on AF Contract No. AF 04(611)-9572, AFRPL-TR-66-21, January 1966. MATSCIT PS 66-1, California Institute of Technology.

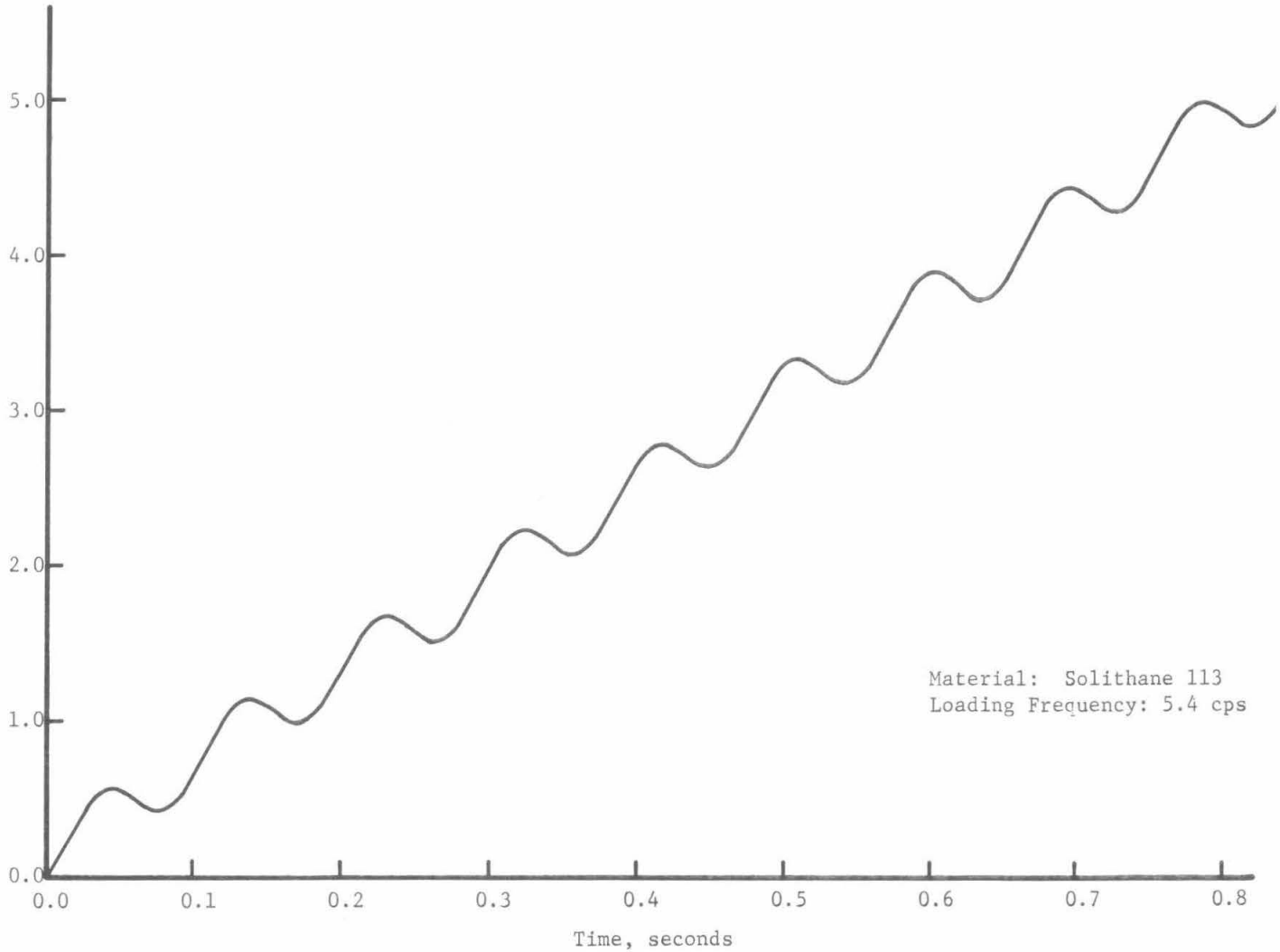

Figure 1. Nonstationary Solution of Thermodynamic Power Equation for Linearly Viscoelastic Material (Equation 15).

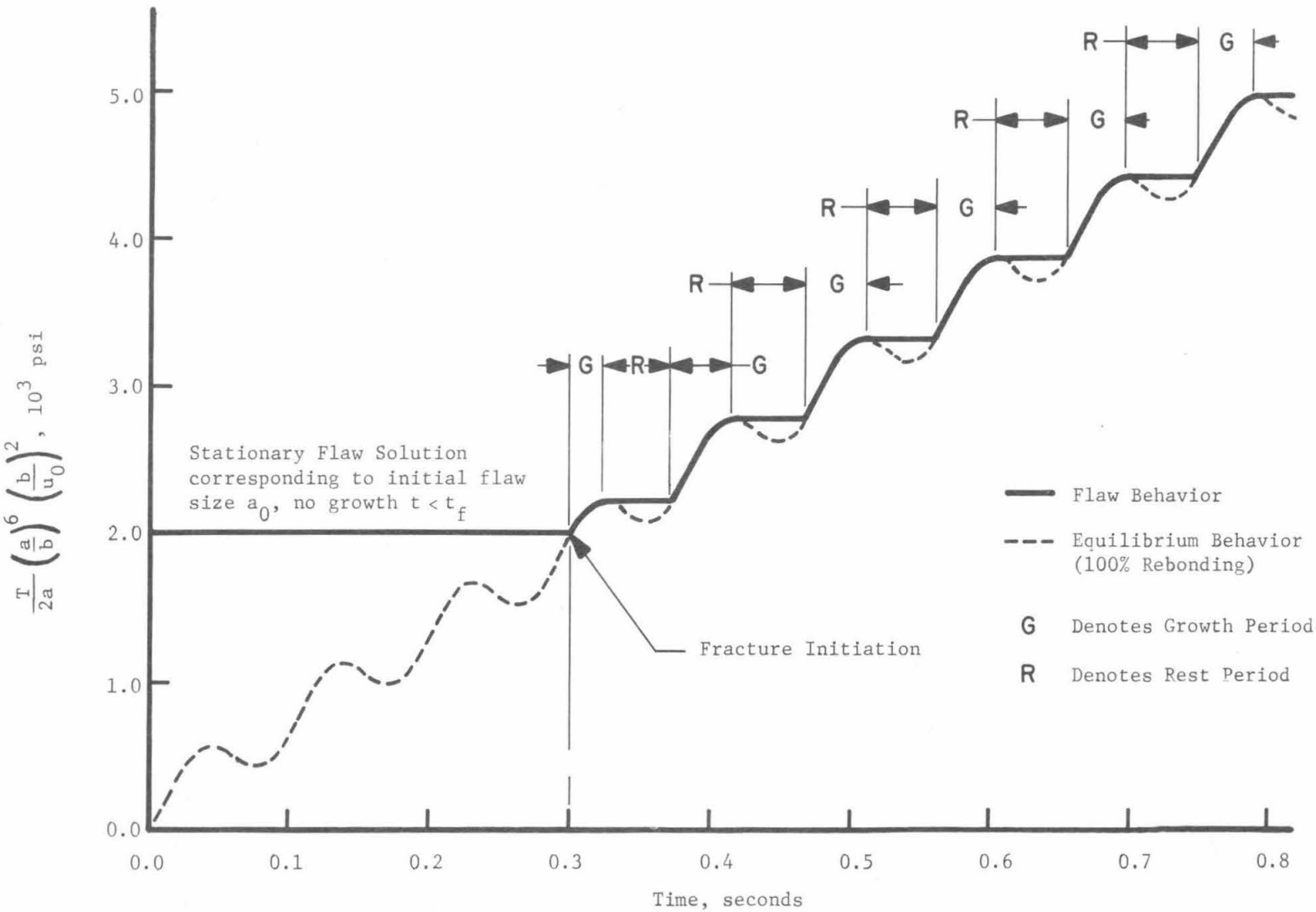

Figure 2. Growth of Spherical Flaw due to Oscillatory Displacement $u = u_0 \sin \omega t$ (Solithane 113, 5.4 cps).

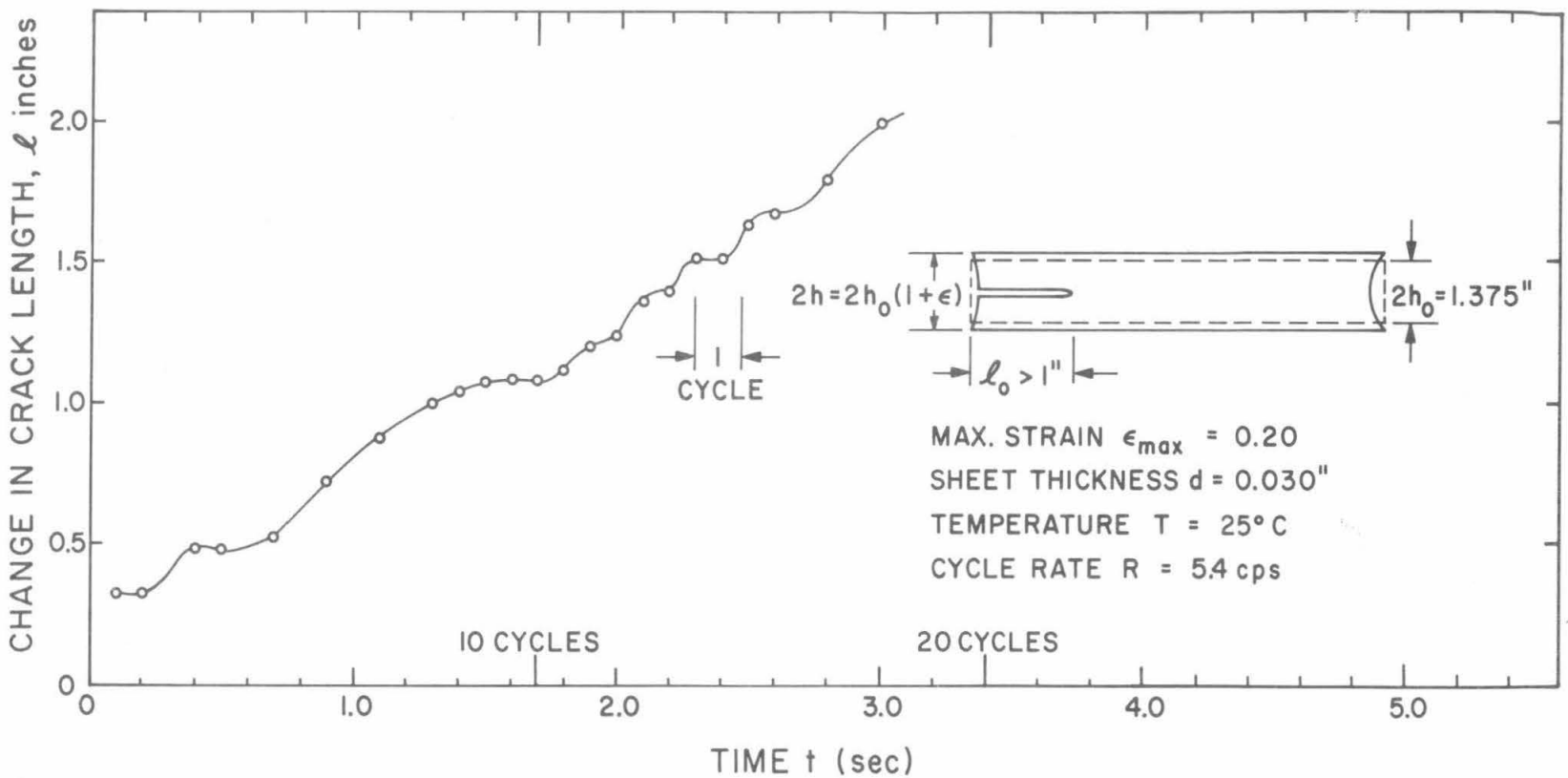

Figure 3. Growth History of a Crack in a Sinusoidally Varying Strain Field (Maximum strain $\varepsilon_{max} = 0.20$).

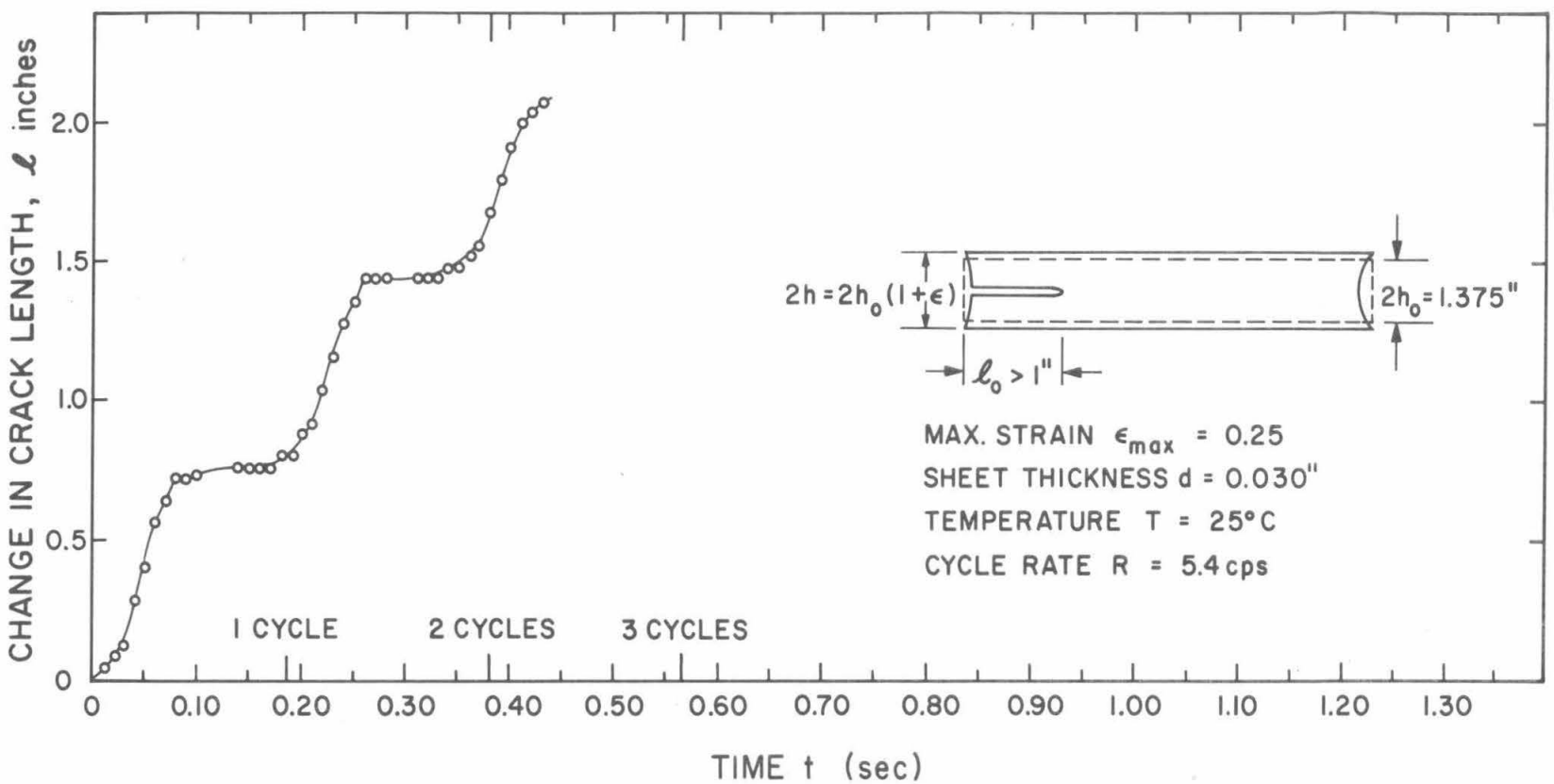

Figure 4. Growth History of a Crack in a Sinusoidally Varying Strain Field (Maximum strain $\varepsilon_{max} = 0.25$).

UNCLASSIFIED
Security Classification

DOCUMENT CONTROL DATA - R&D

(Security classification of title, body of abstract and indexing annotation must be entered when the overall report is classified)

1. ORIGINATING ACTIVITY *(Corporate author)*
Chemical Propulsion Information Agency
Applied Physics Lab., Johns Hopkins Univ.
8621 Georgia Ave., Silver Spring, Md. 20910

2a. REPORT SECURITY CLASSIFICATION
UNCLASSIFIED

2b. GROUP

3. REPORT TITLE
Interagency Chemical Rocket Propulsion Group: Working Group on Mechanical Behavior - 5th Meeting, Vol. I

4. DESCRIPTIVE NOTES *(Type of report and inclusive dates)*

5. AUTHOR(S) *(Last name, first name, initial)*

6. REPORT DATE	7a. TOTAL NO. OF PAGES	7b. NO. OF REFS
October 1966	720	

8a. CONTRACT OR GRANT NO.	9a. ORIGINATOR'S REPORT NUMBER(S)
NOw 62-0604-c	CPIA Publication 119, Vol. I
b. PROJECT NO.	
c.	9b. OTHER REPORT NO(S) *(Any other numbers that may be assigned this report)*
d.	

10. AVAILABILITY/LIMITATION NOTICES In addition to security requirements which must be met, this document is subject to special export controls and each transmittal to foreign governments or foreign nationals may be made only with the prior approval of the Naval Air Systems Command: AIR-330.

11. SUPPLEMENTARY NOTES	12. SPONSORING MILITARY ACTIVITY
	Naval Air Systems Command(AIR-330) Dept. of the Navy Washington, D.C. 20360

13. ABSTRACT

Unclassified complete papers accepted for, and available prior to, the fifth meeting of the ICRPG Working Group on Mechanical Behavior (of solid propellants) are presented. The papers relate to four broad areas: (1) relationship between microstructure and propellant mechanical properties, (2) new or improved experimental methods for characterization, (3) failure criteria, and (4) structural analysis.

DD FORM 1 JAN 64 1473

UNCLASSIFIED
Security Classification

14. KEY WORDS	LINK A		LINK B		LINK C	
	ROLE	WT	ROLE	WT	ROLE	WT
Solid propellants						
Mechanical behavior						
Stress-strain analysis						
Grain design						
Structural failure criteria						
Filled polymers						
Binder-filler interaction						
Fracture modes						
Test methods						
Viscoelastic materials						
Solid propellant grains						

INSTRUCTIONS

1. ORIGINATING ACTIVITY: Enter the name and address of the contractor, subcontractor, grantee, Department of Defense activity or other organization *(corporate author)* issuing the report.

2a. REPORT SECURITY CLASSIFICATION: Enter the overall security classification of the report. Indicate whether "Restricted Data" is included. Marking is to be in accordance with appropriate security regulations.

2b. GROUP: Automatic downgrading is specified in DoD Directive 5200.10 and Armed Forces Industrial Manual. Enter the group number. Also, when applicable, show that optional markings have been used for Group 3 and Group 4 as authorized.

3. REPORT TITLE: Enter the complete report title in all capital letters. Titles in all cases should be unclassified. If a meaningful title cannot be selected without classification, show title classification in all capitals in parenthesis immediately following the title.

4. DESCRIPTIVE NOTES: If appropriate, enter the type of report, e.g., interim, progress, summary, annual, or final. Give the inclusive dates when a specific reporting period is covered.

5. AUTHOR(S): Enter the name(s) of author(s) as shown on or in the report. Enter last name, first name, middle initial. If military, show rank and branch of service. The name of the principal author is an absolute minimum requirement.

6. REPORT DATE: Enter the date of the report as day, month, year; or month, year. If more than one date appears on the report, use date of publication.

7a. TOTAL NUMBER OF PAGES: The total page count should follow normal pagination procedures, i.e., enter the number of pages containing information.

7b. NUMBER OF REFERENCES: Enter the total number of references cited in the report.

8a. CONTRACT OR GRANT NUMBER: If appropriate, enter the applicable number of the contract or grant under which the report was written.

8b, 8c, & 8d. PROJECT NUMBER: Enter the appropriate military department identification, such as project number, subproject number, system numbers, task number, etc.

9a. ORIGINATOR'S REPORT NUMBER(S): Enter the official report number by which the document will be identified and controlled by the originating activity. This number must be unique to this report.

9b. OTHER REPORT NUMBER(S): If the report has been assigned any other report numbers *(either by the originator or by the sponsor)*, also enter this number(s).

10. AVAILABILITY/LIMITATION NOTICES: Enter any limitations on further dissemination of the report, other than those imposed by security classification, using standard statements such as:

(1) "Qualified requesters may obtain copies of this report from DDC."

(2) "Foreign announcement and dissemination of this report by DDC is not authorized."

(3) "U. S. Government agencies may obtain copies of this report directly from DDC. Other qualified DDC users shall request through _____."

(4) "U. S. military agencies may obtain copies of this report directly from DDC. Other qualified users shall request through _____."

(5) "All distribution of this report is controlled. Qualified DDC users shall request through _____."

If the report has been furnished to the Office of Technical Services, Department of Commerce, for sale to the public, indicate this fact and enter the price, if known.

11. SUPPLEMENTARY NOTES: Use for additional explanatory notes.

12. SPONSORING MILITARY ACTIVITY: Enter the name of the departmental project office or laboratory sponsoring *(paying for)* the research and development. Include address.

13. ABSTRACT: Enter an abstract giving a brief and factual summary of the document indicative of the report, even though it may also appear elsewhere in the body of the technical report. If additional space is required, a continuation sheet shall be attached.

It is highly desirable that the abstract of classified reports be unclassified. Each paragraph of the abstract shall end with an indication of the military security classification of the information in the paragraph, represented as *(TS), (S), (C), or (U)*.

There is no limitation on the length of the abstract. However, the suggested length is from 150 to 225 words.

14. KEY WORDS: Key words are technically meaningful terms or short phrases that characterize a report and may be used as index entries for cataloging the report. Key words must be selected so that no security classification is required. Identifiers, such as equipment model designation, trade name, military project code name, geographic location, may be used as key words but will be followed by an indication of technical context. The assignment of links, roles, and weights is optional.